Original Article

54

INDONESIAN SCHOLAR SOCIETY

Indones. J. Chem. Stud.
2026, 5(1), 54–61
Available online at journal.solusiriset.com
e-ISSN: 2830-7658; p-ISSN: 2830-778X

Indonesian Journal of Chemical Studies

Synthesis and Characterization of SnO and SnO_2 Catalysts for Biodiesel from Crude Palm Oil via Interesterification

Amadea Kenyoning Hapsari Subiakto[1], M. Sulthon Nurharmansyah Putra[1]*, Dewi Anggraini Septaningsih[1], Hanifah Setya Ningrum[1], Fikriyah Hamidah[1], Ardine Kusuma Nismarawati[1], Zaidan Al Fajri[1], Maura Agnes Erwinda[1]

[1]*Department of Chemistry, The Republic of Indonesia Defense University, Bogor 16810, Indonesia*

Received: 12 Sep 2026; Revised: 4 May 2026; Accepted: 12 Jun 2026;
Published online: 30 Jun 2026; Published regularly: 30 Jun 2026

Abstract— This study reports the synthesis and characterization of SnO and SnO_2 catalysts for biodiesel production from crude palm oil (CPO) via interesterification. SnO was synthesized using the hydrothermal method, while SnO_2 was prepared through the sol–gel route. The catalysts were applied in the interesterification of refined bleached palm oil with methyl acetate at an oil : methyl acetate molar ratio of 1:9, catalyst loading of 0.25 wt%, reaction temperature of 65 °C, and reaction time of 3 h. X-ray diffraction (XRD) analysis confirmed the formation of tetragonal SnO and rutile tetragonal SnO_2 phases. Biodiesel quality was evaluated according to SNI 7182:2015 parameters. Biodiesel produced using SnO showed density of 861 kg/m³, viscosity of 3.09 cSt, water content of 0.25%, free fatty acid (FFA) of 0.66%, and iodine value of 44.04. Meanwhile, SnO_2-catalyzed biodiesel exhibited density of 886 kg/m³, viscosity of 3.12 cSt, water content of 0.22%, FFA of 0.56%, and iodine value of 36.03. GC–MS analysis identified methyl oleate as the dominant compound in SnO-catalyzed biodiesel, while methyl palmitate was dominant in SnO_2-catalyzed biodiesel. These results indicate that both catalysts have potential as alternative heterogeneous catalysts for biodiesel production from palm oil via interesterification.

Keywords— *Biodiesel; Crude Palm Oil; Interesterification; SnO and SnO_2*

1. INTRODUCTION

The continuous increase in global energy demand is driven by economic growth, industrialization, and population expansion. In Indonesia, fossil fuel consumption has grown by an average of 1.3% annually from 2011 to 2022 [1]. This dependence on fossil fuels poses significant challenges, particularly for developing countries, since fossil energy sources are finite and non-renewable. Therefore, energy diversification has become an essential long-term strategy to ensure sustainable energy security by expanding the use of renewable energy sources [2]. Among various alternatives, biodiesel has emerged as a promising renewable and environmentally friendly energy source.

Biodiesel, a long-chain fatty acid methyl ester (FAME), is typically produced from renewable feedstocks such as vegetable oils, animal fats, and algae. It offers several advantages over petroleum-based diesel, including lower emissions of carbon monoxide, carbon dioxide, hydrocarbons, and particulate matter [3]. Indonesia is one of the world's largest producers of crude palm oil (CPO), providing significant potential for biodiesel production. Palm oil contains up to 45–50% oil in its fruit mesocarp, with national production reaching 48.4 million tons in 2019 [4]. In addition to reducing greenhouse gas emissions, biodiesel has strategic importance in the defense sector, where its application in transportation and tactical equipment may reduce reliance on imported fossil fuels and strengthen national energy resilience.

The production of biodiesel generally involves transesterification and interesterification reactions, both of which require catalysts to enhance reaction efficiency. Heterogeneous catalysts are of particular interest due to their ease of separation and reusability [5]. Various heterogeneous catalysts have been reported for biodiesel production, including MgO–CaO/SiO_2 [6], ZnO/CaO [7], and $Al(HSO_4)_3$ [8]. Compared to conventional heterogeneous catalysts such as CaO, MgO–CaO, and ZnO/CaO, tin-based catalysts offer distinct advantages, including higher structural stability and improved resistance to leaching during reaction. In addition, SnO and SnO_2 exhibit surface acidity that can facilitate ester formation through Lewis acid mechanisms. These properties make Sn-based catalysts promising alternatives for biodiesel production, particularly in interesterification systems where catalyst stability and acid functionality are crucial.

Although heterogeneous catalysts such as CaO, MgO–CaO, and ZnO/CaO have been widely studied, their application is often limited by issues such as catalyst leaching and reduced stability during reaction. In contrast, the use of tin-based oxides in crude palm oil

***Corresponding author**.
Email address: m.shultonnp@gmail.com
DOI: 10.55749/ijcs.v5i1.98

interesterification remains relatively unexplored in the context of biodiesel production. Therefore, investigating the comparative catalytic performance of SnO and SnO_2 provides a new perspective for developing more stable and effective catalysts for biodiesel production.

SnO and SnO_2 can be synthesized via different methods, such as hydrothermal and sol-gel techniques, respectively. Hydrothermal synthesis promotes crystal growth under high temperature and pressure conditions [9], while the sol-gel route enables the formation of inorganic compounds at relatively low temperatures through colloid-to-gel phase transformation [10]. These synthesis methods yield catalysts with distinct particle sizes, surface areas, and catalytic properties, which in turn affect biodiesel production efficiency and FAME quality [11].

This study investigates the catalytic performance of SnO and SnO_2 in the interesterification of crude palm oil for biodiesel production. The objectives are to synthesize and characterize SnO and SnO_2 catalysts prepared through hydrothermal and sol-gel methods and to evaluate their catalytic activity in producing fatty acid methyl esters (FAME) via interesterification. The outcomes are expected to provide valuable insights into catalyst design for biodiesel applications and contribute to the development of sustainable renewable energy strategies that support national defense energy security.

2. EXPERIMENTAL SECTION

2.1. Materials

The materials used include $SnCl_2{\cdot}2H_2O$ precursor (98% purity, Aldrich) NaOH (99% purity, Merck), NH_4OH (Merck), ethanol pro analysis (96% purity, Aldrich), distilled water, Crude Palm Oil (CPO) (from PT.SM), methyl acetate, phosphoric acid, and bleaching earth.

2.2. Instrumentations

The instruments used for characterization were XRD Shimadzu MAXima_X XRD-7000 and GC-MS Agilent 7890.

2.3. Synthesis of SnO Catalyst

The tin oxide catalyst was prepared by the hydrothermal methode. Precursor $SnCl_2{\cdot}2H_2O$ was dissolved in pro analysis ethanol and stirred for 3 hours at 25°C. The SnO catalyst was then synthesized by adding the 0.4 M NaOH solution dropwise into the 0.1 M $SnCl_2{\cdot}2H_2O$ solution under continuous stirring. The pH was adjusted to an optimal value of 12. The resulting mixture was subjected to hydrothermal treatment at 180°C for 2 hours using a hydrothermal reactor. The resulting precipitate was dried in an oven at 105°C for 4 hours. After drying, a pale yellow tin oxide powder was obtained.

2.4. Synthesis of SnO_2 Catalyst

The synthesis of SnO_2 began by dissolving $SnCl_2{\cdot}2H_2O$ in ethanol p.a. The mixture was stirred using a magnetic stirrer for 60 minutes in a beaker until a colorless solution was obtained. Ammonia solution (NH_4OH) was added dropwise until a colloidal suspension formed and the pH reached 8. The colloid was separated by centrifugation, and the resulting precipitate was filtered using filter paper and washed twice with a small amount of deionized water. The washed precipitate was dried at 90°C for 3 hours, followed by calcination at 600°C for 2 hours to remove residual solvents and obtain a dry SnO_2 material. The final SnO_2 catalyst was stored in a sealed container to prevent contamination.

2.5. Purification Crude Palm Oil

By degumming proces, the purification of Crude Palm Oil (CPO) using phosphoric acid (H_3PO_4) (0,1% v/w) as a chemical agent. At 80°C for approximately 2 hours stirred with magnetic stirrer. The mixture is then centrifuged at 3,000 rpm for 15 minutes, resulting in degummed CPO. Next, the bleaching process was performed to remove the color from the degummed CPO using bleaching earth. Bleaching earth (BE) is added at 1.5% of the weight of the degummed CPO. The mixture was stirred with a magnetic stirrer for approximately 1 hour at 80°C. After the bleaching process, the mixture was centrifuged at 3,000 rpm for 30 minutes result the Refinery Bleached Palm Oil (RBPO) or purified CPO.

2.6. Interesterification Reaction

The first stage of the interesterification process involves several preliminary calculations to determine the ratio between RBPO and methyl acetate, set at 1:9. The catalyst used in the interesterification process amounted to 0.25% of the total weight of the combined methyl acetate and RBPO. RBPO was first added into the interesterification reactor, followed by the catalyst (SnO or SnO_2), and finally the methyl acetate. The reaction mixture was stirred for 3 hours at a constant temperature of 65°C. After the interesterification process was completed, the resulting biodiesel was centrifuged for 30 minutes at a speed of 3,000 rpm. The supernatant from the centrifugation process was separated and collected as FAME (Fatty Acid Methyl Esters).

3. RESULT AND DISCUSSION

3.1. Hydrothermal Synthesis of SnO Catalyst

The SnO catalyst was successfully synthesized by hydrothermal method. The precursor $SnCl_2{\cdot}2H_2O$ was reacted with NaOH in ethanol, followed by hydrothermal treatment and drying. During the initial stage, the dropwise addition of NaOH into the $SnCl_2{\cdot}2H_2O$ solution led to the formation of a white precipitate, identified as $Sn(OH)_2$, through a reversible precipitation reaction in **Eq. (1)**. Maintaining the solution pH at ~12 was crucial to drive the equilibrium toward $Sn(OH)_2$ formation and to stabilize the intermediate phase before hydrothermal conversion [12].

$$SnCl_2 \cdot 2H_2O(aq) + 2NaOH(aq) \rightleftarrows Sn(OH)_2(s) + 2NaCl(aq) + 2H_2O(l) \quad (1)$$

Under hydrothermal conditions, $Sn(OH)_2$ underwent a dehydration process to form crystalline SnO in **Eq. (2)**.

The closed autoclave system provided high temperature and pressure, promoting particle nucleation, crystal growth, and phase stabilization. This condition allowed amorphous $Sn(OH)_2$ to reorganize into a more ordered SnO structure with improved crystallinity, consistent with previous reports on hydrothermal tin oxide synthesis [13].

$$Sn(OH)_2\,(s) \xrightarrow{\Delta} SnO\ (s) + H_2O\ (l) \quad (2)$$

Morphological transformation during the hydrothermal process is illustrated in **Fig. 1**, where $Sn(OH)_2$ particles gradually converted into SnO nuclei, followed by continuous crystal growth and aggregation into well-organized structures. This sequential growth mechanism explains the improved particle uniformity and enhanced crystallinity observed in hydrothermal-synthesized SnO compared to conventional precipitation or sol-gel methods [14]. The role of SnO as a catalyst lies in its semiconductor properties, providing active sites that facilitate redox reactions by lowering the activation energy of the interesterification process. This is crucial for enhancing both the activity and selectivity in the conversion of RBPO into methyl esters. In this synthesis, NaOH not only acted as a precipitating agent but also functioned as a pH stabilizer, ensuring the controlled formation of $Sn(OH)_2$ and its subsequent transformation into SnO.

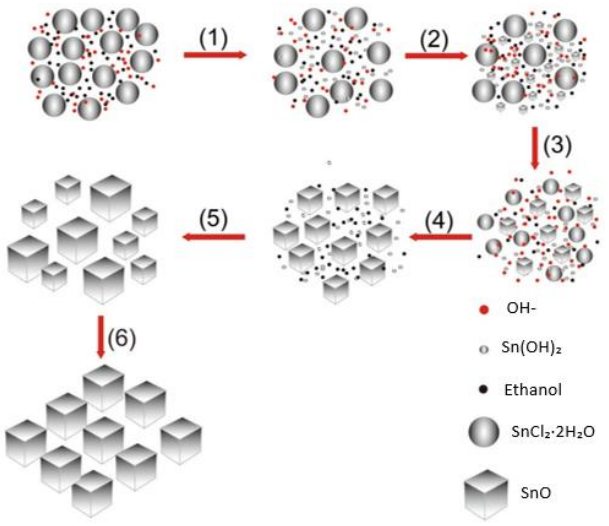

Fig. 1 Schematic of hydrothermal process in SnO synthesis

3.2. Sol-Gel Synthesis of SnO_2 Catalyst

SnO_2 catalyst was successfully synthesized using the sol–gel method with $SnCl_2{\cdot}2H_2O$ as the precursor dissolved in ethanol. Ethanol acted as a solvent that controlled the reaction rate and ensured homogeneous mixing [15]. Controlled addition of ammonia raised the pH, inducing hydrolysis of Sn^{2+} to $Sn(OH)_2$ in **Eq. (3)**. The process yielded a white colloidal sol, which gradually underwent condensation reactions, forming oligomers and subsequently a three-dimensional gel network [16].

$$SnCl_2 \cdot 2H_2O(aq) + 2NH_4OH(l) \rightarrow Sn(OH)_2(s) + 2NH_4Cl(l) + 2H_2O(l) \quad (3)$$

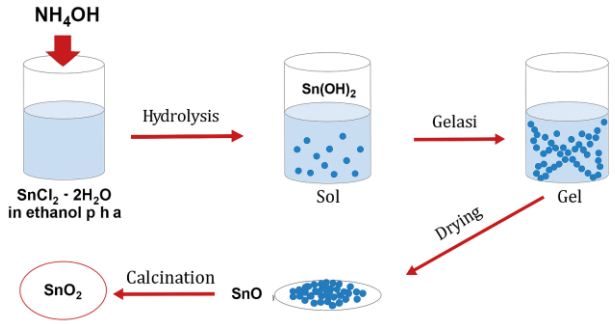

Fig. 2 Schematic diagram of sol-gel process in SnO_2 synthesis

As the hydrolysis progressed, condensation reactions occurred simultaneously, where hydroxyl groups bonded to each other, producing oligomers and eventually forming an interconnected three-dimensional gel network. This transformation from sol to gel is a crucial stage in the sol–gel method, where small clusters of hydroxides aggregate into a porous structure [16]. The process is visualized in **Fig. 2**, where dispersed particles in the sol gradually interconnect, leading to gelation. The resulting gel exhibited a rigid matrix structure but still contained a large fraction of trapped solvent.

The drying step at 90 °C for 3 h allowed the removal of residual ethanol and water, accompanied by the dehydration of $Sn(OH)_2$ to SnO in **Eq. (4)**. At this stage, the dried product appeared as a pale yellowish powder, indicating partial oxidation of Sn species. The structural transformation during drying also resulted in the collapse of some gel pores, while preserving the overall three-dimensional network.

$$Sn(OH)_2(s) \rightarrow SnO(s) + H_2O\ (g) \quad (4)$$

The final stage was calcination, which played a dual role: eliminating volatile compounds and promoting phase transformation from amorphous tin oxide to crystalline SnO_2. During heating, SnO was oxidized to SnO_2 as represented in **Eq. (5)**. This process not only increased crystallinity but also stabilized the oxide structure, producing a white crystalline powder with enhanced structural definition [17]. The calcination step is therefore essential in tailoring the physicochemical properties of SnO_2, particularly its crystallinity and thermal stability, which strongly influence catalytic performance.

$$SnO(s) + \frac{1}{2}O_2(g) \rightarrow SnO_2(s) \quad (5)$$

3.3. Sol-Gel Synthesis of SnO_2 Catalyst

The degumming process successfully removed impurities (gum) consisting of phosphatides, proteins, hydrocarbons, carbohydrates, water, heavy metals, free fatty acids (FFA), tocopherols, pigments, and other minor components from crude palm oil (CPO) [18]. The method applied was acid degumming, where 0.1%

phosphoric acid was added to CPO followed by heating. The addition of phosphoric acid plays a crucial role in converting non-hydratable phosphatides into hydratable forms, thereby enabling more efficient separation in the subsequent step. Separation of gum, oil, and water was then enhanced through centrifugation at 3,000 rpm for 15 minutes.

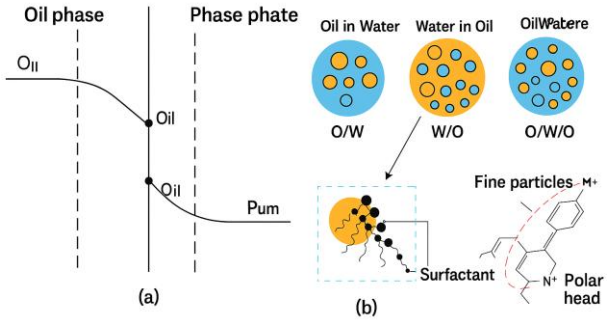

Fig. 3 Interphase diagram (a) and illustration of degumming mechanism (b)

The mechanism of mass transfer in acid degumming can be explained by interphase theory (**Fig. 3**). Gum initially dissolved in the oil phase (liquid phase I) migrates toward the interface and subsequently moves into the phosphoric acid phase (liquid phase II). The interaction between these two phases triggers a chemical reaction that converts non-hydratable phosphatides into hydratable ones, thus facilitating their removal from the oil [19]. This indicates that the efficiency of degumming strongly depends on the degree of contact between the phases.

The next stage is bleaching, a process of decolorization using bleaching earth (BE). BE has the chemical composition $Al_2O_3 \cdot 4SiO_2 \cdot nH_2O$ with silicon (Si), aluminum (Al), and iron (Fe) as its main components. This process aims to reduce undesirable pigments and adsorb other contaminants, thereby improving the overall quality of the oil [20]. Furthermore, the porous structure of BE enhances its ability to trap large molecules, including pigments and other impurities [21].

3.4. Characterization of SnO and SnO_2 Catalysts

The X-ray diffraction (XRD) testing was conducted to identify the crystalline properties of the synthesized SnO catalyst prepared by hydrotermal method and SnO_2 catalyst prepared y sol-gel method. Through this testing, the crystal structure, crystalline phase formed, and purity of each compound could be determined using X-ray radiation [22]. Both samples exhibited diffraction patterns consistent with reference JCPDS data, confirming the successful synthesis of tetragonal SnO (JCPDS 06-0395) and rutile tetragonal SnO_2 (JCPDS 41-1445) (**Fig. 4**).

For SnO, the main characteristic peaks were observed at 2θ = 26.42° (hkl 101), 33.20° (200), and 51.52° (211). The diffractogram indicated broadened peaks, suggesting relatively small crystallite sizes. The crystallinity degree of SnO was calculated as 42%, indicating a partially crystalline structure with remaining amorphous content. Using the Scherrer equation, the crystallite size of SnO was determined in the range of 30.91–176.2 nm, depending on the reflection plane.

In contrast, SnO_2 exhibited sharper and more intense peaks at 2θ = 26.67° (110), 33.95° (101), and 51.85° (211), with additional minor peaks at 37.99°, 54.82°, and 57.92°. This indicates a higher ordering of the crystal lattice. The crystallinity degree of SnO_2 reached 67%, significantly higher than that of SnO (**Table 1**). Crystallite sizes estimated via Scherrer equation were in the range of 181.5–201.55 nm, which reflects larger and more ordered crystal growth compared to SnO.

The difference in crystallinity and crystallite size can be attributed to the synthesis methods: hydrothermal treatment for SnO tends to produce smaller crystallites with lower crystallinity due to incomplete crystal growth, while the sol-gel method followed by calcination for SnO_2 facilitates nucleation and growth of larger and more ordered crystals.

Table 1. Comparison of XRD results for SnO and SnO_2

Catalyst	2θ Peaks (°)	hkl Planes	Crystallinity (%)	Crystallite Size (nm, Scherrer)
SnO	26.42	(101)	42	30.91 –176.2
	33.20	(200)		
	51.52	(211)		
SnO_2	26.67	(110)	67	181.5 – 201.55
	33.95	(101)		
	37.99	(200)		
	51.85	(211)		
	54.82	(220)		
	57.92	(310)		

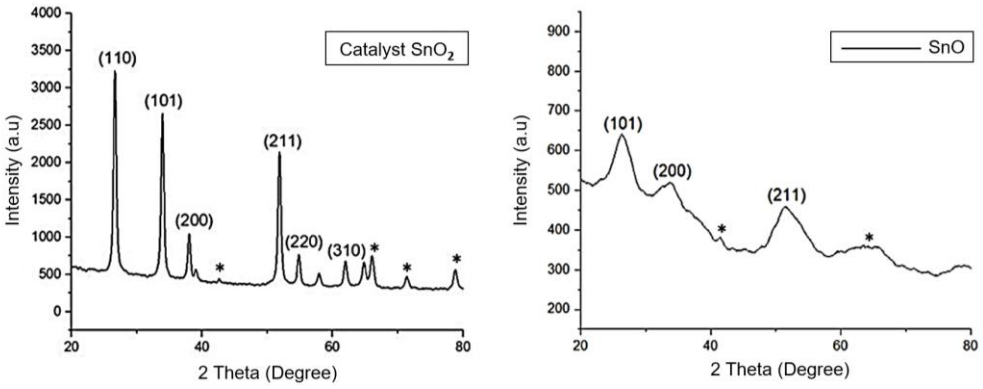

Fig. 4 XRD diffractograms of SnO_2 (left) and XRD diffractograms of SnO (right)

Based on the data in **Table 1** and **Fig. 4**, it can be explained that the XRD results indicate both SnO and SnO_2 were successfully synthesized with crystalline phases corresponding to their standard references. However, SnO_2 showed superior crystallinity and larger crystallite sizes compared to SnO. Higher crystallinity of SnO_2 implies better lattice ordering, which is favorable for catalytic activity due to enhanced surface stability and well-defined active sites. On the other hand, the smaller crystallite size of SnO may provide a higher surface area but at the expense of lower crystallinity. These structural differences suggest that SnO_2 is more suitable for reactions requiring stable and well-ordered catalytic sites, while SnO may contribute through higher dispersion of active sites due to its smaller crystallites.

3.5. Interesterification of Biodiesel

Interesterification is an alternative to transesterification for biodiesel production, with the advantage of producing triacetin instead of glycerol as a by-product [23]. The formation of triacetin instead of glycerol represents an advantage of the interesterification route due to its potential value as a fuel additive. **Fig. 5** illustrates the reaction between triglycerides and methyl acetate proceeds through three reversible steps, forming monoacetin, diacetin, and ultimately triacetin, while releasing methyl esters. In this study, SnO and SnO_2 served as catalysts, which are essential for enhancing reaction efficiency under milder conditions by activating the carbonyl groups of triglycerides and methyl acetate. SnO promotes ester formation through surface –OH interactions, while SnO_2 utilizes Sn^{4+} Lewis acid sites to increase electrophilicity, facilitating acyl exchange and yielding renewable esters suitable as biodiesel [24].

The oils produced using SnO and SnO_2 catalysts showed several observable physical characteristics such as color, odor, viscosity, clarity, and freezing point. The oil from the SnO catalyst appeared dark yellow, while the one from SnO_2 was lighter yellow. Both samples had a distinctive methyl acetate odor and showed no significant differences in viscosity and clarity—both were thinner and clearer than the original RBPO. Based on freezing point observations, the oil derived using SnO tended to solidify more easily at room temperature compared to the SnO_2-derived oil.

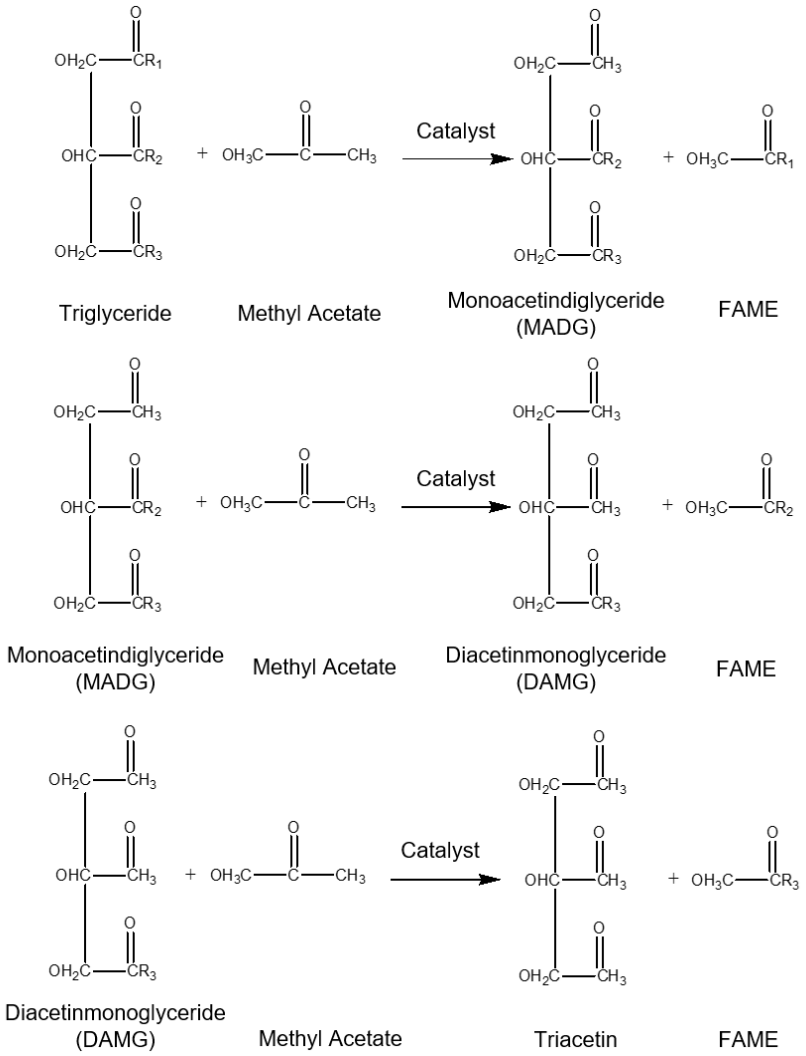

Fig. 5 Mechanism of interesterification reaction

3.6. Analysis GC-MS of Biodiesel

Gas Chromatography–Mass Spectrometry (GC–MS) is an analytical technique that combines gas chromatography (GC) and mass spectrometry (MS) to identify and analyze volatile compounds in complex samples. In biodiesel characterization, GC–MS is applied to identify and classify fatty acid methyl esters (FAME) based on their fragmentation patterns [26]. In this study, the analysis was performed using a GC–MS Agilent 7890 instrument.

For the SnO catalyst, the main identified compound was 9-octadecenoic acid methyl ester (methyl oleate), detected at a retention time of 20.883 minutes with a similarity index of 93% and peak area contribution of 0.32%. Methyl oleate is a monounsaturated fatty acid ester, which is commonly present in biodiesel and contributes to good ignition quality and lubricity.For the SnO_2 catalyst, several compounds were detected, including hexadecanoic acid methyl ester (methyl palmitate) with a retention time of 19.227 minutes, similarity index of 97%, and peak area of 1.29% (**Table 2**). Other minor compounds such as propanoic acid methyl ester and didehydro-9-ketoabietic acid were also observed. The dominance of saturated FAME such as methyl palmitate indicates that SnO_2 catalyzed reactions favor the formation of more stable biodiesel components with higher oxidative resistance.

Table 2. Comparison of GC–MS identified compounds in biodiesel from SnO and SnO_2 catalyst

Catalyst	Retention Time (min)	Compound Name	% Area	% Qual	Remarks
SnO	20.883	9-Octadecenoic acid methyl ester (Methyl oleate)	0.32	93	Unsaturated FAME, improves lubricity
SnO_2	19.227	Hexadecanoic acid methyl ester (Methyl palmitate)	1.29	97	Saturated FAME, improves oxidative stability

Based on the data GC–MS results show that both SnO and SnO_2 catalysts successfully facilitated the formation of fatty acid methyl esters from RBPO. However, the product distribution varied significantly. SnO predominantly yielded unsaturated FAME such as methyl oleate, while SnO_2 favored the formation of saturated FAME such as methyl palmitate, with higher peak intensity. This difference reflects the catalytic nature of each oxide: SnO, with Sn^{2+} active sites, promotes reactions involving unsaturated fatty acids, while SnO_2, with stronger Lewis acidic Sn^{4+} sites, provides a more efficient pathway for acyl exchange, suggesting improved catalytic activity and stability of products. Consequently, SnO_2 tends to generate biodiesel with improved oxidative stability, whereas SnO-derived biodiesel is enriched in unsaturated esters that enhance lubricity. The GC–MS peak area values represent relative compound abundance and were not used to determine biodiesel yield.

3.7. Biodiesel Fuel Properties

The physicochemical properties of biodiesel produced using SnO and SnO_2 catalysts were evaluated based on SNI 7182:2015 standards (**Table 3**). Biodiesel obtained using SnO showed density of 861 kg/m³, viscosity of 3.09 cSt, water content of 0.25%, and free fatty acid (FFA) content of 0.66%. Meanwhile, biodiesel produced using SnO_2 exhibited density of 886 kg/m³, viscosity of 3.12 cSt, water content of 0.22%, and FFA content of 0.56%. Both products showed acceptable density and viscosity values, while SnO_2 demonstrated slightly better fuel quality due to lower water and FFA contents. Although the FFA value of SnO_2 slightly exceeds the SNI limit, it remains close to the acceptable range and indicates partial conversion of free fatty acids. Overall, SnO_2 exhibited slightly better fuel properties than SnO.

Table 3. Biodiesel physicochemical properties from SnO and SnO_2 catalyst

Properties	SnO	SnO_2	SNI 7182:2015
Density (kg/m^3)	861	886	850-890
Viscosity (cSt)	3.09	3.12	2.3-6.0
Water (%)	0.25	0.22	≤0.6
FFA (%)	0.66	0.56	≤0.5

Although quantitative biodiesel yield was not determined in this study, catalyst performance could be comparatively evaluated through fuel property measurements and GC–MS analysis. The detection of methyl ester compounds confirms successful interesterification, while lower water and FFA values for SnO_2 indicate better product quality.

4. CONCLUSION

SnO and SnO_2 catalysts were successfully synthesized and applied in crude palm oil interesterification. Both catalysts produced biodiesel with acceptable physicochemical properties. SnO_2 showed better product quality in terms of lower water content and free fatty acid values, while GC–MS confirmed methyl ester formation for both catalysts. Further characterization using techniques such as FTIR, BET, and SEM/TEM is recommended to provide more comprehensive insights into catalyst properties. Overall, tin oxide catalysts demonstrate potential as alternative heterogeneous catalysts for biodiesel production.

5. AUTHOR'S DECLARATION

5.1. Supporting Information

There is no supporting information in this paper. The data that support the findings of this study are available on request from the corresponding author (ES).

5.2. Acknowledgements

The experimental work was carried out at the Integrated Chemistry Laboratory, Republic of Indonesia Defense University.

5.3. Conflict of Interest

The authors declared that no conflicts of interest regarding the publication of this article. The authors confirm that the paper is free of plagiarism.

5.4. Author Contributions

AKHS and MSNP conducted the experiment and analyzed data. HSN, FH, AKN, and ZAF conducted the interesterification calculations, DAS revised the manuscript. All authors agreed to the final version of this manuscript.

5.5. AI Statement

ChatGPT was utilize to enhance the clarity, grammar, and overall readability of this manuscript. All technical content, data interpretation, and conclusion were solely developed and verified by the authors. The final version of the manuscript was thoroughly reviewed to ensure accuracy, coherence, and aligment with the study's findings.

6. REFERENCES

[1] Yudiartono, Y., Windarta, J. and Adiarso, A. 2022. Analisis prakiraan kebutuhan energi nasional jangka panjang untuk mendukung program peta jalan transisi energi menuju karbon netral. *JEBT*. *3*(3). 201-217. Doi: https://doi.org/10.14710/jebt.2022.14264

[2] De Rosa, M., Gainsford, K., Pallonetto, F. and Finn, D.P. 2022. Diversification, concentration and renewability of the energy supply in the European Union. *Energy*. *253*. 124097. Doi: https://doi.org/10.1016/j.energy.2022.124097

[3] Devita, L. 2015. Biodiesel sebagai bioenergi alternatif dan prospeftif. *Agrica Ekstensia*. *9*(2). 23-26.

[4] Murgianto, F., Edyson, E., Ardiyanto, A., Putra, S.K. and Prabowo, L. 2021. Potential content of palm oil at various levels of loose fruit in oil palm circle. *Jurnal Agro Ind. Perkeb.* 91-98. Doi: https://doi.org/10.25181/jaip.v9i2.2161

[5] Abbas, G.H. and Ilyas, N.M. 2021. Review: penggunaan katalis heterogen pada produksi biodiesel. *Jurnal Ilmiah Kimia dan Pendidikan Kimia*. *22*(2). 99-107. Doi: https://doi.org/10.35580/chemica.v22i2.26406

[6] Widayat, W., Maheswari, N.T., Fitriani, W., Buchori, L., Satriadi, H., Kusmiyati, K. and Ngadi, N. 2023. Preparation of MgO-CaO/SiO 2 catalyst from dolomite and geothermal solid waste for biodiesel production. *Int. J. Renew. Energy Dev*. *12*(3). 541. Doi: https://doi.org/10.14710/ijred.2023.51573

[7] Wicaksono, D. and Kusumaningtyas, R.D., 2019. Synthesis of ZnO/CaO catalyst from eggshell waste for biodiesel production. *JBAT*. *8*(1). 65-71. Doi: https://doi.org/10.15294/jbat.v8i1.20185

[8] Welter, R.A., Santana, H.S., Gaziola de la Torre, L., Barnes, M.C., Taranto, O.P. and Oelgemöller, M. 2023. Biodiesel Production by Heterogeneous Catalysis and Eco-friendly Routes. *ChemBioEng Rev*. 10(2). 86–111. Doi: https://doi.org/10.1002/cben.202200062

[9] Namratha, K., Nayan, M.B., Darshan, M.S., Basavarajappa, H.T., Madesh, P. and Byrappa, K. 2022. Hydrothermal–From Geology to Technology (Part 1). *J. Geol. Soc. India*. *98*(3). 353-362. Doi: https://doi.org/10.1007/s12594-022-1987-0

[10] Muslim, I., Safrihatini, W. and Aini, W. 2017. Pengaruh katalis pada proses pembentukan partikel nano silika sebagai material hidrofobik. *JKPK*. *2*(3). 152-157. Doi: https://doi.org/10.20961/jkpk.v2i3.11920

[11] Elgharbawy, A.S., Sadik, W., Sadek, O.M. and Kasaby, M.A. 2021. A review on biodiesel feedstocks and production technologies. *Chil. Chem. Soc*. *66*(1). 5098-5109. Doi: http://dx.doi.org/10.4067/S0717-97072021000105098

[12] Husein, S., Wahyuni, E.T. and Mudasir, M. 2019. Synthesis of Tin (II) Oxide (SnO) nanoparticle by hydrothermal method. *JKPK*. *4*(3). 145-151. Doi: https://doi.org/10.20961/jkpk.v4i3.29898

[13] Zhang, Y., Zhong, L. and Duan, D. 2016. A single-step direct hydrothermal synthesis of SrTiO3 nanoparticles from crystalline P25 TiO2 powders. *J. Mater. Sci*. *51*(2). 1142-1152. Doi: https://doi.org/10.1007/s10853-015-9445-7

[14] Niu, Y.Q., Liu, J.H., Aymonier, C., Fermani, S., Kralj, D., Falini, G. and Zhou, C.H. 2022. Calcium carbonate: controlled synthesis, surface functionalization, and nanostructured materials. *Chem. Soc. Rev*. *51*(18). 7883-7943. Doi: https://doi.org/10.1039/D1CS00519G

[15] Murzalinov, D., Dmitriyeva, E., Lebedev, I., Bondar, E.A., Fedosimova, A.I. and Kemelbekova, A. 2022. The effect of pH solution in the sol–gel process on the structure and properties of thin SnO2 films. *Processes*. *10*(6). 1116. Doi: https://doi.org/10.3390/pr10061116

[16] Katoueizadeh, E., Rasouli, M. and Zebarjad, S.M. 2020. A comprehensive study on the gelation process of silica gels from sodium silicate. *J. Mater. Res. Technol.* 9(5). 10157–10165. Doi: https://doi.org/10.1016/j.jmrt.2020.07.020

[17] Wahyuningsih, F., Wahyudi, B.S., Teguh, A. and Sri, W. 2016. Kinetika Kalsinasi Seria Zirkonia dari Proses Gelasi Eksternal. *Jurnal Rekayasa Proses*. *10*(1). 16-22. Doi: https://doi.org/10.22146/jrekpros.34423

[18] Rossani, W.I. and Amri, A., 2021. Penentuan Kadar bleaching earth dan Phosporic acid pada Proses Degumming dan bleaching crude palm oil. *J. Bioprocess, Chem. Environ. Eng. Sci. 2*(2). 1–14. Doi: https://doi.org/10.31258/jbchees.3.1.1-14

[19] Ristianingsih, Y., Sutijan, S. and Budiman, A. 2012. Studi Kinetika Proses Kimia Dan Fisika Penghilangan Getah Crude Plam Oil (Cpo) Dengan Asam Fosfat. *Reaktor*. *13*(4). 242-247. Doi: https://doi.org/10.14710/reaktor.13.4.242-247

[20] Hasballah, T. and Siregar, L.H. 2021. Analisa pemakaian jumlah BE (bleaching earth) terhadap kualitas warna DBPO (Degummed Bleached Palm Oil) pada tangki bleacher (d202) dengan kapasitas 2000 Ton/Hari di unit refinery PT. SMART Tbk Belawan. *J. Teknol. Mesin UDA*. *1*(1). 9–16.

[21] Veronika, N. and Sihotang, A., 2023. Pengaruh Bleaching Earth Pada Proses Pemucatan Terhadap Kualitas Produksi Minyak Goreng Sawit (Palm Olein). *J. Sains dan Ilmu Terap. 6*(1). 36–42. Doi: https://doi.org/10.59061/jsit.v6i1.140

[22] Hakim, L., Dirgantara, M. and Nawir, M. 2019. Karakterisasi struktur material pasir bongkahan galian golongan c dengan menggunakan X-Ray Difraction (X-RD) di kota Palangkaraya. *Jurnal Jejaring Matematika dan Sains*. *1*(1). 44-51. Doi: https://doi.org/10.36873/jjms.v1i1.136

[23] Agusti, T.R., Agustine, D. and Nurlatifah, I. 2020. Esterifikasi Gliserol Produk Samping Biodiesel Menjadi Triasetin Menggunakan Katalis SO42-/TiO2. *JIMTEK*. *1*(3), 290-297.

[24] Daryono, E.D. 2020. Proses Interesterifikasi Minyak Kelapa Sawit Menjadi Biodiesel Dengan Co-solvent Metil Ester. *Jurnal Rekayasa Bahan Alam dan Energi Berkelanjutan*. *4*(1). 1-8. Doi: https://doi.org/10.21776/ub.rbaet.2020.004.01.01

[25] Tefera, N.T., Nallamothu, R.B., Alemayehu, G. and Kefale, Y. 2024. Optimization, characterization, and GC-MS analysis of CSOME produced using alkali catalyzed transesterification. *Energy Convers. Manag.: X*. *22*, 100549. Doi: https://doi.org/10.1016/j.ecmx.2024.100549